

# Prediction of Grain Size in Cast Aluminum Alloys

Shuai Ma <sup>1,2,3</sup>, Zhibo Zhang <sup>2,3,\*</sup>, Zhuming Huang <sup>2,3,4</sup>, Dongfu Song <sup>2,3</sup>, Yiwang Jia <sup>2,3</sup>, Nan Zhou <sup>2,3</sup>, Kai Wang <sup>4</sup>, Kaihong Zheng <sup>2,3,\*</sup> and Huijing Du <sup>1,\*</sup>

<sup>1</sup> Key Laboratory for Microstructural Material Physics of Hebei Province, School of Science, Yanshan University, Qinhuangdao 066004, China; mashuai1215@ysu.edu.cn

<sup>2</sup> Institute of New Materials, Guangdong Academy of Sciences, Guangzhou 510651, China; huangzhuming@gdinm.com (Z.H.); songdongfu@gdinm.com (D.S.); jiayiwang@gdinm.com (Y.J.); zhounan@gdinm.com (N.Z.)

<sup>3</sup> Guangdong Provincial Key Laboratory of Metal Toughening Technology and Application, Guangzhou 510561, China

<sup>4</sup> School of Mechatronic Engineering and Automation, Foshan University, Foshan 528001, China; hfutwk927@fosu.edu.cn

\* Correspondence: zhangzhibo@gdinm.com (Z.Z.); zhengkaihong@gdinm.com (K.Z.); hjdu@ysu.edu.cn (H.D.)

**Abstract:** Grain refinement of cast alloys, especially aluminum–silicon and magnesium-based alloys, is an effective approach to improve the strength of alloys. Grain size is the most representative parameter used to characterize grain refinement in the industry, thereby attracting increasing attention for developing accurate grain size prediction models. In this paper, several important grain size prediction models under different adaptation conditions are reviewed. These models are obtained either by regression of experimental data or by physical/mathematical inference under certain assumptions of specified cases, focusing on the effects of alloy composition, solidification temperature gradient, grain growth rate, and fining agent composition, among others. The trends of grain size prediction models were also discussed. The results revealed machine learning as an effective tool to establish a data-driven prediction model of grain size in cast aluminum alloys.

**Keywords:** grain size; prediction model; alloy composition; aluminum alloys



**Citation:** Ma, S.; Zhang, Z.; Huang, Z.; Song, D.; Jia, Y.; Zhou, N.; Wang, K.; Zheng, K.; Du, H. Prediction of Grain Size in Cast Aluminum Alloys. *Crystals* **2022**, *12*, 474. <https://doi.org/10.3390/cryst12040474>

Academic Editors: Sergio Brutti and Bolv Xiao

Received: 25 January 2022

Accepted: 11 March 2022

Published: 29 March 2022

**Publisher's Note:** MDPI stays neutral with regard to jurisdictional claims in published maps and institutional affiliations.



**Copyright:** © 2022 by the authors. Licensee MDPI, Basel, Switzerland. This article is an open access article distributed under the terms and conditions of the Creative Commons Attribution (CC BY) license (<https://creativecommons.org/licenses/by/4.0/>).

## 1. Introduction

The development of lightweight alloys is important to save energy and reduce emissions [1]. Aluminum is an important metal in the industry with total consumption coming just after that of steel due to its abundant resources [2]. Aluminum is widely used in various fields, such as transportation, construction, aviation, aerospace, navigation, and medical. Magnesium is one of the lightest engineering metal raw materials, with high specific stiffness, good damping and cutting, easy to recycle and other advantages. Magnesium has been widely used in electronic communications, automotive transportation, military and other industrial fields. Therefore, the performance requirements for aluminum and magnesium alloys have become increasingly stringent. Meanwhile, the processing technology of alloys is also upgrading with the development of related industries [3–5]. For industrial production, grain refinement is economical since it can greatly improve the strength of aluminum and its alloys, reduce casting defects, such as porosity, and increase the quality of wrought alloys. Thus, the grain refinement of alloys has become an active research topic in the past couple of decades [6].

According to the metal solidification nucleation theory, currently available grain refinement techniques of alloys can be divided into two basic approaches [7,8]. The endogenous nucleation method is based on the thermal-mechanical treatment of solid Al alloys, leading to an increased number of effective spontaneous nucleation or inhibition of grain size growth to achieve grain refinement. The other approach is based on the external nucleation particle method used to achieve grain refinement during the casting

process by adding metal grain refiners to metal melting to obtain enough heterogeneous nuclei during solidification. Compared to endogenous nucleation, the heterogeneous nucleation method has become the most common and economical route for the production of aluminum due to its simple processing and the fact that it does not require special equipment and has a better refinement effect [7,8], such as the superheating method, the Elfinal process [9] and carbon inoculation [10]. On the other hand, the development of highly accurate and realistic grain size prediction models is highly desirable to solve the shortcomings of the grain size refinement method that is mostly used in the industry [11].

Various specific grain size prediction models have been developed to date under different adaptation conditions. The models have mainly been based on two types: (i) empirical models obtained by the experimental data regression and (ii) theoretical models developed by physical or mathematical inference under certain conditions and assumptions.

In this article, the empirical and theoretical models used for grain size prediction are reviewed, including the solute elements, solidification temperature gradient, grain growth rate, and potent nucleant effects on grain refinement, as well as different grain refining theories and models. With the rapid development of computational materials science, machine learning (ML) has emerged as a new method to predict material parameters based on local theoretical research and an experimental dataset [12]. Researchers have achieved good results in predicting material properties by machine learning, such as predicting the fatigue strength of steel, the crystallinity of molecular materials, new stable materials, the enthalpy of formation and the interfacial mismatch of compounds [13,14]. Therefore, based on the dataset and theoretical study of alloy material parameters, the prediction of grain size of alloy materials by machine learning will become the future development trend in material informatics.

## 2. Empirical Model

### 2.1. The Growth Restriction Factor

Grain refinement is beneficial in terms of improving the soundness of aluminum products, reducing hot tearing susceptibility, declining homogenization time, and improving its mechanical properties [15]. In the process, nucleation substrates provide heterogeneous sites for primary solid phase nucleation at low supercooling, while solute elements offer compositional supercooling for restricting grain growth and facilitating nucleation. The solute element  $C_0$  was the first included factor in the classical supercooling criterion by Tiller et al. [16]. Maxwell and Hellawell [17] were the first to consider the solute  $C_0$  as an independent alloy parameter relevant to the grain refinement of Al alloys [17]. The solute element  $C_0$  emerged from Maxwell and Hellawell's [17] simple model of grown spherical crystals and was restricted by the partitioning of a single solute into a binary alloy. This can be expressed by Equation (1):

$$R = \lambda_s(D_1t)^{1/2} \quad (1)$$

where  $R$  represents the radius of the sphere,  $D_1$  refers to the diffusion coefficient of the solute in the liquid,  $t$  denotes the time, and  $D_1 = f(S)$ .

$S$ , known as the growth parameter, can be given by Equation (2):

$$S = \frac{2(C_1 - C_0)}{C_S - C_1} = \frac{2\Delta T_c}{m_1 C_0(k - 1) - \Delta T_c(k - 1)} \quad (2)$$

where  $C_S$  and  $C_1$  are the compositions of the solute element in the solid and liquid phases, respectively;  $m_1$  is the gradient of the liquidus slope and  $k$  is the partition coefficient.

By assuming that thermal gradient is zero without thermal subcooling, the corresponding temperature profile showing the constitutionally undercooled zone,  $\Delta T_c$ , can be calculated according to Equation (3) (As shown in Figure 1):

$$\Delta T_c = T_{le} - T_{actual} = m_1(C_0 - C_1) \quad (3)$$

where  $T_{actual}$  is the equilibrium liquidus temperature and  $T_{le}$  is the actual temperature in the melt.

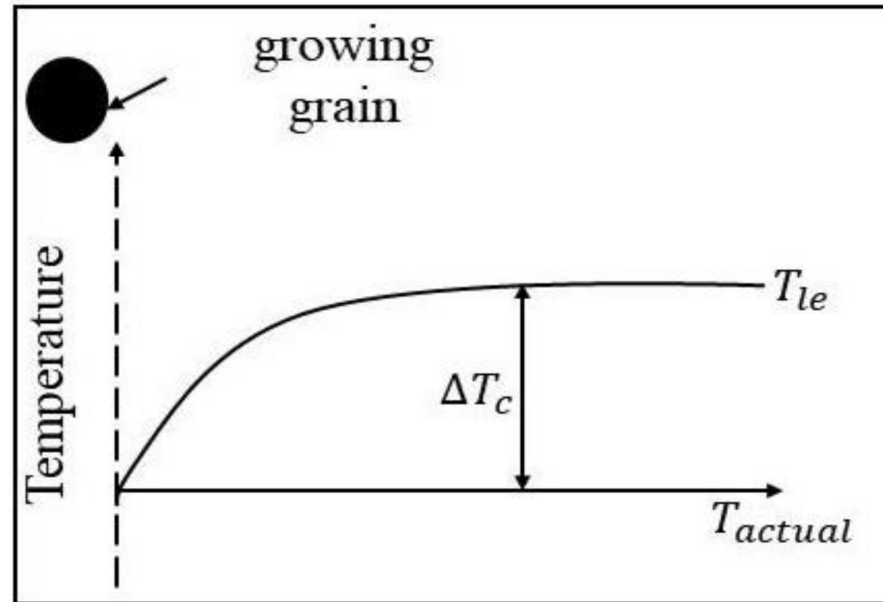


**Figure 1.** A representation of the constitutive undercooled zone in front of the growing equiaxed grains obtained by assuming no contribution from thermal subcooling or latent heat, as well as a negligible thermal gradient ( $T_{actual}$  is a constant value). Figures taken from Acta Metallurgica [17] with permission.

By assuming the zero diffusion of solute in the solid phase and instantaneous diffusion of solute in the liquid phase, Equation (4) can be obtained:

$$C_1 = \frac{C_0}{(1 - f_s)^P}, \quad P = 1 - k \quad (4)$$

The injection of Equation (4) into Equation (3) yields Equation (5):

$$\Delta T_c = m_1 C_0 \left( 1 - \frac{C_0}{1 - (1 - f_s)^P} \right) \quad (5)$$

At  $f_s = 1$ ,

$$\Delta T_c = \frac{m_1 C_0 (k - 1)}{k}$$

The initial constitutional subcooling rate of development can be defined according to Equation (6):

$$\frac{d\Delta T_c}{df_s} = - \frac{m_1 C_0 P}{(1 - p f_s)^2}, \quad \text{where } p = 1 - k \quad (6)$$

At  $f_s = 0$ , the growth restriction factor,  $Q$ , can be given by Equation (7):

$$Q = m C_0 (k - 1) \quad (7)$$

The growth restriction factor  $Q$  has been obtained for magnesium [6] and aluminum [5] alloys in the literature. Easton et al. [11] selected eight wrought aluminum alloys with a variety of alloy elements and the growth restriction factor  $Q$  to determine the grain size prediction [5]. The results indicate the growth restriction factor  $Q$  is very reliable regarding the grain size and  $1/Q$  is a close fit to a linear relationship within a scatter of

approximately 10 to 20 pct [5]. With the introduction of the growth restriction factor, the effect of different alloy composition on the grain refinement of cast magnesium alloys has attracted extensive interest from researchers and a number of new grain refiners have been developed. Zirconium, with a high GRF [5] ( $Q = 38.29$ ), was reported to be the most successful and effective grain refining agent known for magnesium; the first commercially available alloy of zirconium material was produced in 1945 and was called Zirmax [5]. The growth restriction factor  $Q$  value of calcium in a Mg alloy is 11.94, which is only second to zirconium in magnesium alloys [18]. The grain size reduction rate of 28.5–45% was observed when appropriate amounts of calcium elements were added to molten magnesium [19,20]. Therefore, the new grain refiner alloys were developed by exploring the principles of grain refinement of growth limiting factors.

The growth restriction factor  $Q$  can be used for any binary alloy system to describe the influence of main factors on grain size and evaluate the actual average size of the alloy, which has been adopted by the most of researchers [5]. However, the model does not suggest why the nucleants present in the melt nucleate. The nucleation that occurs in front of the interface remains unresolved [21] and the model is only suitable for binary alloy systems.

## 2.2. The Relative Grain Size Grain

The relative grain size model assumes that the nucleation of the grain is mainly determined by the subcooling of free nucleation in the metal solution without the refiner or when the effect of the refiner ion is not strong. To generate free nucleation subcooling for the formation of next grains on an adjacent nucleation substrate, the grain must grow to a specific size, representing another indirect expression of grain size. Easton et al. [22] developed an equation to calculate grain size using the relative grain size model shown by Equation (8):

$$R_{GS} = 1 - \left( \frac{m_1 C_0}{m_1 C_0 - \Delta T'_n} \right)^{1/k-1} \quad (8)$$

where  $\Delta T'_n$  is the critical subcooling of the free-form nucleus,  $m_1$  represents the liquidus slope,  $C_0$  refers to the solute content, and  $k$  is the equilibrium partition coefficient.

The relative grain size reflects the solid fraction of previous grain growth when the next grains were nucleated. The results show that smaller  $R_{GS}$  led to a smaller grain size and  $R_{GS}$  was mainly related to the critical subcooling of grain nucleation. For larger critical subcooling, the formation of new grains was difficult. The results show that when  $R_{GS}$  is small, the grain size is smaller and  $R_{GS}$  is mainly related to the critical subcooling of grain nucleation. On the contrary, when the critical subcooling degree  $\Delta T'_n$  is smaller or  $\Delta T'_n = 0$ , it indicates that the existing grain core does not require component subcooling for nucleation. At that moment, the growth of previous grains was greatly limited to zero, and grain size was the same as that of the actual grain core.

The relative grain size is not the absolute value of grain size. The relative grain size model is based on the assumption that nucleant substrates are activated by the constitutional undercooling generated by the growth of an adjacent grain, indicating the grain size varies on addition of solute and nucleant particles. The model was established by D.H. Stijon [22] and the relative grain size for a range of grain refiner additions to pure aluminum and an  $AlSi_7Mg_{0.3}$  alloy were predicted. For pure Al, the addition of titanium as a solute resulted in a significant reduction in grain size. For the  $AlSi_7Mg_{0.3}$  alloy, the reduction in grain size was slight with the addition of titanium as a solute. In both cases, the addition of stronger nucleating agents (lower values of  $\Delta T_n$ ) was also effectively reduce the grain size and the predicted results are compared with the actual grain size data obtained experimentally, which correlate well with the observations in the literature [23,24].

The model can be used for any binary alloy system, but for multi-component alloys, it can be calculated using the undercooling calculated at the specific fraction of solids using the multi-component diagram [5]. The relative grain size was based on the calculation of the growth limitation factor  $Q$ , activating the adjacent nucleation particle requiring

an undercooling for the nucleation of  $\Delta T_n$ . The model considered the latent heat release due to the crystallization of equiaxed grains (which creates a small negative gradient at the interface and the positive temperature gradient due to the extraction of the mold for positive temperature gradients or casting, and thus it can be understood why a wave of nucleation events occurs from the mold walls toward the center of the melt) [5]. However, the model ignores latent heat and thermal gradients, although the model does assume that each grain needs to grow to produce the next grain required for the constitutive overcooling to the core. However, both latent heat and positive thermal gradients reduce the amount and size of the subcooling zone in front of the interface, which may require more constitutive subcooling.

### 2.3. The Semi-Empirical Model

Easton et al. [22] also proved the importance of the growth restriction factor  $Q$  in controlling and forging the quality of the alloy by the effects of Al-3Ti-1B refiners on the grain size of eight cast aluminum alloys. The previous studies revealed that the effect of the added refiner and alloy content on grain size can be well predicted [25–30]. To characterize and quantify the effects of nucleant particles on grain size, the contribution of solute content must be established. Easton et al. [22] experimentally obtained specific expressions for grain size at a cooling rate of 1 °C/s using Equation (9):

$$d = \frac{32}{\sqrt[3]{\varphi(\text{TiB}_2)}} + \frac{652}{Q} \quad (9)$$

where  $\varphi(\text{TiB}_2)$  is the volume fraction of  $\text{TiB}_2$  particles (a phase in the refiner) in the aluminum solution. The factor  $a$  is a constant related to the number of nucleated substrates (or amount of refiner added), and  $b$  is a constant related to the nucleate base capability.

Using the same principle, Lee et al. [31] developed a relationship for the Al5Ti1B grain refiner:

$$d = \frac{43}{\sqrt[3]{\varphi(\text{TiB}_2)}} + \frac{520}{Q} \quad (10)$$

The coefficient values in Equations (9) and (10) were used to define the nucleation characteristics of a particular type of grain refiner. The size of the constants  $a$  and  $b$  changes due to the different refiners [30]. At low solute contents, the alloys obtained by Lee et al. [31] were identified as superior master alloys. At high solute content levels, the alloys by Easton et al. [22] were characterized as better intermediate alloys [22]. This kind of analysis may provide a tool to understand grain refinement more effectively.

On the other hand, the cooling rate  $V$  should be included in the grain size prediction model since the cooling rates may differ and easily vary in actual production [26]. Easton et al. [22] suggested a formula after adding the Al-3Ti-1B refiner to the aluminum alloys of eight different solutes under various cooling rates. The expression obtained after testing the grain size can be written as Equation (11) [32]:

$$d = \frac{1}{\sqrt[3]{f(R)N_v}} + \frac{b'\Delta T_n}{QR^{1/2}} \quad (11)$$

where  $f(R)$  represents the fraction of effective nucleation substrates on all nucleation substrates, related to the cooling rate.  $N_v$  refers to the volume fraction of all shaped nucleated substrates in the Al alloy liquid.  $b'$  is a constant and  $R$  refers to the cooling rate;  $\Delta T_n$  denotes the critical subcooling degree for free growth on the substrate of the fining agent particles; and  $d$  represents the diffusion coefficient of the solute [29].

The critical subcooling degree of the refiner particles  $\Delta T_n$  for free growth on the substrate can be expressed by Equation (12):

$$\Delta T_n = \frac{4\sigma}{\Delta S_v d} \quad (12)$$

where  $\sigma$  is the solid–liquid interfacial tension of the liquid phase in the alloy,  $\Delta S_v$  refers to the volume entropy of liquid metal, and  $d$  is the particle diameter of the fining agent.

Compared to Equation (9), the influence of the subcooling rate on grain size was considered in Equation (10). Note that smaller grain sizes would be obtained at larger cooling rates. The experimental [22] results showed that the semi-empirical model can provide a further understanding of the mechanism of grain refinement. Zr poisoning and the addition of silicon of more than 3% [33] can also lead to grain refinement. The semi-empirical model assisted to determine the mechanism of the grain refinement effect of the Zr and Si elements on the AlTiB master alloy. The change of solidification conditions will significantly change grain size and the simulation of different solidification processes showed that each experiment produced different grain sizes.

Easton et al. [22] summarized the formula of the semi-empirical model:

$$d = \frac{a}{\sqrt[3]{\varphi(d)}} + \frac{b}{Q} \quad (13)$$

where  $\varphi(d)$  is the volume fraction in the alloy,  $a$  is a constant related to the number of nucleation substrates (the amount of grain fining agent addition), and  $b$  is a constant related to the nucleation capacity of the nucleation substrates. The semi-empirical model will be strengthened by obtaining data for a greater range of cooling rates. The semi-empirical model generates substantial amounts of thermal undercooling, and it will encourage the nucleation of many grains adjacent to the walls of the casting cavity.

The semi-empirical model has been found to be applicable to aluminum and magnesium alloys [28], having a broad applicability in many alloy systems. However, the model assumes that the nucleation of grains occurs due to the constitutional cooling mechanism inside the melt because it does not take into account the effect of the wall crystals formed due to the insufficient thermal cooling of the casting walls.

### 3. Theoretical Model

#### 3.1. Free-form Nucleation Grain Size Model

The component subcooling effect at the grain subcooling degree, reaching the critical nucleation subcooling, would yield a spontaneous nucleation process based on free nucleation. The process of spontaneous nucleation was based on free nucleation at the grain subcooling degree reaching the critical nucleation subcooling due to the composition subcooling. The free-form nucleation grain size model was proposed by Qian and Stjohn based on the analysis of nucleation caused by composition subcooling [26].

The free-form nucleation grain size model assumes that grain formation is the result of the interdependence between nucleation and growth within an environment dictated by the alloy chemistry [34]. The grain size  $d_{gs}$  of the microstructure is determined by three components: (i) the distance at which a previously nucleated grain must grow; (ii) the distance of the diffusion field from the S–L interface to the end of the field; and (iii) the additional distance to the nearest most potent nucleant particle. It can be seen from Figure 2 that the grain size ( $d_{gs}$ ) of the microstructure can be expressed as [34]:

$$d_{gs} = x_{cs} + x'_{dl} + x_{sd} \quad (14)$$

The estimation of  $x'_{dl}$  requires knowledge of the solute distribution ahead of the S–L interface. For alloys with a solute composition of  $C_0$  forming the crystal nucleus from the liquid phase, the crystal nucleus can be regarded as spherical due to the small crystal nucleus. The accumulation of solute led to the precipitation of the initial solute component in the liquid phase, which can be estimated to be  $KC_0$ . As solid phase increased, the  $C_s$  line of the solid phase composition changed.

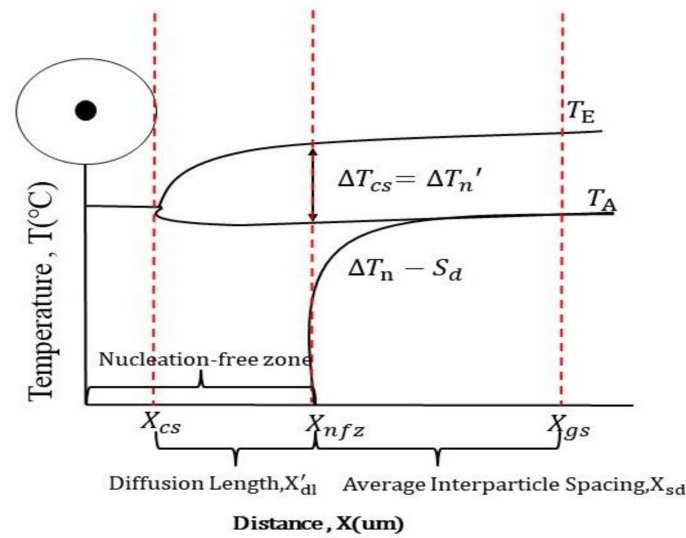


**Figure 2.** Scheme was simplified to show the intersection between the actual temperature  $T_A$  and the  $\Delta T_n - S_d$  curve indicating the location of the nucleation event, and the three regions that together establish the grain size of the microstructure:  $x_{cs}$ ,  $x'_{dl}$  and  $x_{sd}$ . The first two regions  $x_{cs}$  and  $x'_{dl}$  represent a nucleation-free zone, where nucleation is not possible for the particle distribution described by  $\Delta T_n - S_d$ .  $\Delta T'_n$  is the difference between the actual temperature in the melt. Figures taken from Acta Materialia [34] with permission.

On the solid–liquid interface (Figure 3), the solid phase composition is  $(x'_{dl} + x_{sd})$ , representing the liquid phase composition on the solidification interface.  $k$  refers to the equilibrium partition coefficient,  $v$  is the crystal growth rate, and  $D$  denotes the diffusion coefficient of the solute in the liquid phase [35,36].

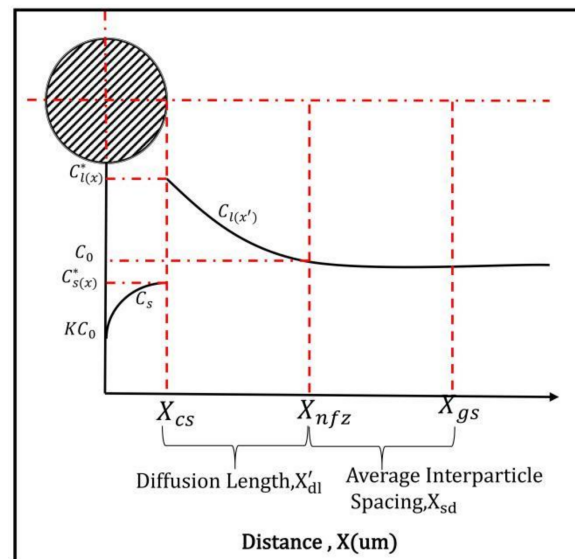


**Figure 3.** The distribution relationship of the solute in the liquid and solid phases during the formation of the grain. Figures taken from Acta Materialia [34] with permission.

Accordingly, Equation (15) can be obtained:

$$C_1^* = \frac{C_s^*(x_{cs})}{k} = \frac{C_0}{k} \left[ 1 - (1 - k) \exp\left(-k \frac{v}{D} (x'_{dl} + x_{sd})\right) \right] \quad (15)$$

The accumulation of the solute led to the formation of an enriched layer in the liquid phase at the solid–liquid interface. As the solute advanced toward the liquid phase by diffusion, it changed in the enriched layer. This can be expressed by Equation (16):

$$C_1(x') = C_0 + (C_1^*(x_{cs}) - C_0) \exp\left(-\frac{v}{D}(x'_{dl} + x_{sd})\right) \quad (16)$$

The liquid phase front forms a compositional subcooling zone due to the solute concentration  $C_1^*(x_{cs}) > C_0$  within the enriched layer.

At the constitutional supercooling,  $\Delta T'_n$ , at some point on the front edge of the liquid phase, equals the critical subcooling required for nucleation,  $x_{cs}$ , and the distance,  $x'_{dl} + x_{sd}$ , between the grain growth front and the next nucleation point can be expressed according to Equation (17):

$$x'_{dl} + x_{sd} = \frac{D\Delta T'_n}{vQ} + x_{sd} \quad (17)$$

Where  $D$  is the diffusion coefficient of solute ( $m^2/s$ ), and  $v$  is the nucleation growth rate ( $m/s$ ).

Stjohn et al. [22] derived the specific expression of  $x_{cs} + x_{sd}$  :

$$x'_{dl} + x_{sd} = \frac{4.6D}{v} \left( \frac{C_1^* - C_0}{C_1^*(1-k)} \right) + x_{sd} \quad (18)$$

The grain size model can be obtained by Equation (19):

$$d_{gs} = \frac{D\Delta T'_n}{vQ} + \frac{4.6D}{v} \left( \frac{C_1^* - C_0}{C_1^*(1-k)} \right) + x_{sd} \quad (19)$$

Since the temperature continually decreased from the wall to the center, the nucleation supercooling required for the grain declines as well. Therefore,  $\Delta T'_n$  can be taken as  $Z\Delta T'_n$  at  $Z < 1$ , ( $Z = 0.1$ ) to yield Equation (20) [22]:

$$d_{gs} = \frac{DZ\Delta T'_n}{vQ} + \frac{4.6D}{v} \left( \frac{C_1^* - C_0}{C_1^*(1-k)} \right) + x_{sd} \quad (20)$$

M. Qian et al. [22] calculated the grain size of Al–Ti and Mg–Al binary alloys. The calculation results showed that a small amount of refiner grains led to nucleation and the ratio remained constant in the Al–Ti alloys. In the Mg–Al alloys, the experimental value of 7217 and the predicted value of 7542 were obtained for commercial purity alloys [34]. The commercial alloy value is very close to the experimental value, indicating that the free-form nucleation grain size model is very reliable in magnesium–aluminum alloys. The free-growth model showed that the wide grain size distribution and the formation of an invisible nucleation zone are the main reasons for the low grain refinement efficiency. Therefore, it is an effective method to improve grain refinement by controlling the growth rate of the alloy and minimizing the nucleation zone.

The free-form nucleation grain size model can provide theoretical guidance for future work on predicting the grain size of cast alloys and answer some questions associated with grain refinement. However, the model also has some limitations in predicting grain sizes variations in a large range because of the inaccuracy or insufficiency of the thermodynamic and diffusion data used in the calculation [34]. The model also cannot explain what type and size of particles are more effective to promote the heterogeneous nucleation and which solute should be added to create the  $C_5$  with the smaller nucleation free zone [34]. Therefore, the free form nucleation grain size model must be used in conjunction with other models in order to develop new and more effective grain refinement processes for cast metals.

### 3.2. Free-Growth Grain Model

In the free-growth grain model, the heterogeneous core formed after the addition of the refiner acts as the crystal nucleus, and crystal particles grow freely without the nucleation process. The addition of refiner grains to the liquid metal incites the refiner particles to directly act as heterogeneous particles to promote the free growth of grains. In this case, the number of free growth particles is considered as the number of particles [37]. After obtaining the grain number  $N(v)$  in unit volume, the average grain size  $d$  can be derived by the expression reported by Gree et al. [33]:

$$d = \sqrt[3]{\frac{0.5}{N(v)}} \quad (21)$$

where  $N(v)$  is the total particles during the growth of the nucleus. For particles with diameter  $d$  grown as a nucleus, the critical subcooling  $\Delta T_{fg}$  can be obtained by Equation (22):

$$\Delta T_{fg} = \frac{4\sigma}{\Delta S_v d} \quad (22)$$

where  $\sigma$  represents the solid–liquid interfacial tension of the liquid phase of the alloy,  $d$  is the particle diameter of the fining agent, and  $\Delta S_v$  refers to the volume entropy of liquid metal.

According to the phase diagram of the alloy and the related theory, the volume fraction  $N(d)$  of the free growth refiner particles can be calculated, and the average grain size  $d$  can be obtained.

The grain radius  $r$  of the spherical growth in isothermal heat can be expressed by Equation (23) [38,39]:

$$r = \lambda_s (D_s t)^{1/2} \quad (23)$$

In this case, the melting point of the alloy is  $T_0$ . At a solute content of  $C_0$  and temperature of  $T_1$  ( $T_0 - T_1 = \Delta T_{fg}$ ) [40], the refiner grains with diameter  $d$  start growing. The growth rate  $v$  can be obtained by Equations (24)–(26):

$$V_s = \frac{\lambda_s^2 D}{2r} \quad (24)$$

$$\lambda_s = \left( \frac{-S}{2\pi^{1/2}} \right) + \left( \frac{S^2}{4\pi} - S \right)^{1/2} \quad (25)$$

$$S = \frac{2(C_{IL} - C_0)}{C_{IS} - C_{IL}} \quad (26)$$

where  $C_{IS}$  is the solute content in the solid–liquid interface, and  $C_{IL}$  refers to the solute content in the liquid at the solid–liquid interface [40].

After time  $dt$  of growth, the size of the particles can be estimated by Equation (27):

$$r_{n+1} = r_n + V dt \quad (27)$$

For crystals grown on particles with diameters  $d$  to  $d + \delta d$ , a heat input  $q(d)\delta d$  is induced into the melt at the  $n$ th increment. At this time, the grain growth releases the latent heat  $q$  total according to Equation (28) [41]:

$$(q(d)\delta d)_n = N(d)\delta d 4\pi r_{n-1}^2 (r_n - r_{n-1}) \Delta H_v \quad (28)$$

where  $\Delta H_v$  is the latent heat of solidification per unit volume.

In each increment, the heat inputs from each group of growing crystals is summed to yield the total  $q$  total, representing the melt temperature in the next interval. This can be given by Equation (29):

$$T_{n+1} = T_n - Rdt + \frac{q_{\text{total}}}{C_{PV}} \quad (29)$$

where  $C_{PV}$  is the specific heat of the melt per unit volume.

If the growth conditions of the refiner particles are not met, Equation (30) is valid:

$$\Delta T = T_{n+1} - T_n < \Delta T_{fg} \quad (30)$$

The above process is then repeated at the critical subcooling, satisfying the growth conditions of the refiner particles according to Equation (31):

$$\Delta T = T_{n+1} - T_n > \Delta T_{fg} \quad (31)$$

In this case, the grain growth releases the latent heat, and grain fraction  $N(d)$  can be obtained by the above formula to yield the average grain size  $d$ .

Men's [42] study showed that the combination of theoretical modelling based on the free growth model elucidates the mechanism of grain refinement by the melt-enhanced shear, and quantitatively studied the initial stage of solidification in the sheared and non-sheared AZ91 alloy melt. Men et al. obtained experimentally for the AZ91 alloy that the maximum volume of the melt was  $157 \text{ cm}^3$  and the measured undercooling rate was  $\sim 0.22 \text{ CS}^{-1}$  near the temperature of the alloy liquid, in the case of the standard TP-1 test with the undercooling rate of  $\sim 3.5 \text{ KS}^{-1}$  and the melt volume of  $\sim 100 \text{ cm}^3$  [42]. The good agreement between the theoretical predictions and the experimental observations suggests that the free-growth grain model is very reliable in magnesium and aluminum alloys. The results of quantitative studies show that the MgO particles in the oxide films are effectively dispersed into more individual particles by intense melt shearing. In this case, the number density of active nucleated particles in the sheared melt increased and achieved significant grain refinement. Therefore, for strong nucleation agents, the nucleation stage itself is not a controlling factor, as the number of grains is determined by free-growth conditions.

The free growth model is neither time dependent nor stochastic and a particle size distribution was applied and can be successfully applied to Al-Ti-B- and Al-Ti-C-based grain refiners [43] inoculated in aluminum alloys and SiC refiners inoculated in magnesium alloys. The model showed that a new crystalline phase could start free growth on the potent particles at an undercooling inversely proportional to the diameter of the nucleating substrate. The largest particles in the melt start to grow first, as soon as the required undercooling is reached, followed by the progressively smaller ones as the undercooling is increased [42]. However, the model only deals with equiaxed growth and therefore may make unrealistic predictions outside. In order to describe the different types of casting and variations in casting conditions, the only input parameter of the model is the cooling rate. It is not sufficient to have only this input parameter for the model, especially in the case of large temperature gradients which will hinder the prediction of the grain size. Therefore, the model is only applicable to the prediction of grain size with equal growth rate.

#### 4. Future Trends for Predicting Grain Size

The above-developed grain size prediction models are characterized by high cost, long lead time, and easy failure. The empirical model ignores latent heat and thermal gradients. Both latent heat and positive temperature gradients reduce the number and size of the subcooling zone at the interface, resulting in small grain diameters obtained. The theoretical model is poorly modeled in experiments with fine grain particles and lacks a quantitative description of the relationship between grain refinement results and important parameters, such as refining agents. Hence, shortening the process of the model from discovery to application is very important. The development of accurate, reliable, convenient, and

applicable grain size prediction models with data support has received increased attention using existing relevant material data and empirical knowledge.

With the development of the advanced data and success achieved by their technologies, machine learning has shown great potential in scientific research [44,45]. For example, Agrawal et al. [12] used information from data analysis tools to build a machine learning model to predict the fatigue strength of steel using the National Institute for Materials Science (NIMS) public domain database and proposed a framework for the systematic end-to-end exploration of materials. Wicker et al. [13] used a support vector machine regression algorithm with radial basis kernel functions for predicting the molecular material crystallinity. Meredig et al. [14] constructed a machine learning model to predict 4500 new stable materials from a database of density generalized function theory (DFT) calculations with 6 orders of magnitude less computational time than DFT. To date, machine learning has been associated with material research to provide new ways for the development of new materials driven by large amounts of data generated by scientific experiments and computational simulations [46]. Therefore, the prediction of the grain size model by machine learning would become an effective means to address the needs of material development in today's society [47,48]. The machine learning method could predict the grain size of aluminum alloys by analyzing large numbers of experimental data and carry out correlation analyses, feature selection, regression analyses, and integrated algorithms [49,50]. In sum, the prediction model of grain size by machine learning would expand the knowledge of grain size in the existing technologies, reduce the blindness of experiments to a certain extent, save time and cost, and enhance the intelligence of enterprise production and service.

## 5. Conclusions

This review introduced the related research on solidification grain size models and predicted future trends in the grain size of alloy materials by machine learning methods. The empirical models are determined by three components. (i) The growth restriction factor  $Q$  is applied to any binary alloy system and is the key quantity for the term effect on grain growth and the grain refinement during alloy solidification. In addition to this, the growth restriction factor  $Q$  evaluates the relative or actual average size of the alloy and has been applied in magnesium and aluminum alloys. However, the model does not suggest why the nucleants are present in the melt nucleate. (ii) The relative grain size model can be used for any binary alloy system, but for multi-component alloys, it can be calculated using the undercooling calculated at the specific fraction of solids using the multi-component diagram. In addition to this, the relative grain size model can explain the occurrence of a wave of nucleation events from the mold walls toward the center of the melt and can predict the size trend of nucleated particles in different solute content ranges. However, the model neglects latent heat and thermal gradients. (iii) The semi-empirical model has been found to be applicable to aluminum and magnesium alloys, having a broad applicability in many alloy system. However, the model assumes that the nucleation of grains occurs due to the constitutional cooling mechanism inside the melt because it does not take into account the effect of the wall crystals formed due to the insufficient thermal cooling of the casting walls.

The theoretical models are determined by two components. (i) The free-form nucleation grain size model can provide theoretical guidance for future works to predict the grain size of cast alloys and answer questions associated with grain refinement. However, the model also has some limitations as it cannot explain what type and size of particles are more effective to promote the heterogeneous nucleation and which solute be added to create a  $C_S$  with a smaller nucleation-free zone. Therefore, the free-form nucleation grain size model must be used with other models. (ii) The free growth model was successfully applied grain refinement of Al-Ti-B- and Al-Ti-C-based grain refiners inoculated in aluminum alloys. However, the model only deals with equiaxed growth and therefore may

make unrealistic predictions outside. The model is only applicable to the prediction of grain size with equal growth rate.

The theoretical and empirical models of grain size can accurately reflect the actual grain size and play an important role in industrial production. The grain prediction model deepens the theoretical understanding of metal solidification conditions and has great scientific importance for future research on grain size refinement. However, they also have corresponding application limitations, and it can be difficult to meet the demand of today's rapid research and development of materials. Therefore, the article first proposed to use machine learning to predict the grain size and improve the grain size prediction model. Machine learning can be used to predict the eigenvalues and grain size of aluminum alloys. With the development of computing technology, the prediction of grain size through machine learning will become the trend of future research.

**Author Contributions:** S.M. wrote the manuscript, designed the entire work and revised the manuscript; Z.Z. conceived the entire conceptualization; Z.H., D.S., N.Z., Y.J. and K.W. helped with investigation and discussed the results; Z.Z., K.Z. and H.D. supervised the entire work. All authors have read and agreed to the published version of the manuscript.

**Funding:** The work was financially supported by Guangdong Province Key Area R and D Program (2020B10186002), Foshan Key Technology Project (1920001000409) and the Key Laboratory of Modern Ceramic and Aluminum Profile Equipment of Guangdong Regular Higher Education (2017KSYS012).

**Institutional Review Board Statement:** Not applicable.

**Informed Consent Statement:** Not applicable.

**Data Availability Statement:** Not applicable.

**Conflicts of Interest:** The authors declare no conflict of interest.

## References

1. Mohanty, P.; Gruzleski, J. Mechanism of grain refinement in aluminium. *Acta Metall. Mater.* **1995**, *43*, 2001–2012. [\[CrossRef\]](#)
2. Cibula, A.; Ruddle, R. The effect of grain size on the tensile properties of high strength cast aluminum alloys. *J. Inst. Met.* **1949**, *76*, 1949–1950.
3. Dahle, A.K.; Tondel, P.A.; Paradies, C.J.; Arnberg, L. Effect of grain refinement on the fluidity of two commercial Al-Si foundry alloys. *Metall. Mater. Trans. A* **1996**, *27*, 2305–2313. [\[CrossRef\]](#)
4. Quedstedt, T.; Greer, A. The effect of the size distribution of inoculant particles on as-cast grain size in aluminium alloys. *Acta Mater.* **2004**, *52*, 3859–3868. [\[CrossRef\]](#)
5. Greer, A.; Bunn, A.M.; Tronche, A.; Evans, P.V.; Bristow, D.J. Modelling of inoculation of metallic melts: Application to grain refinement of aluminium by Al-Ti-B. *Acta Mater.* **2000**, *48*, 2823–2835. [\[CrossRef\]](#)
6. StJohn, D.H.; Qian, M.; Easton, M.A.; Cao, P.; Hildebrand, Z. Grain refinement of magnesium alloys. *Metall. Mater. Trans. A* **2005**, *36*, 1669–1679. [\[CrossRef\]](#)
7. Peng, C.; Qian, M.; StJohn, D.H. Effect of Iron on Grain Refinement of High-Purity Mg-Al Alloys. *Scr. Mater.* **2004**, *51*, 125–129.
8. McCartney, D.G. Grain refining of aluminium and its alloys using inoculants. *Int. Mater. Rev.* **1989**, *34*, 247–260. [\[CrossRef\]](#)
9. Ramirez, A.; Qian, M.; Davis, B.; Wilks, T.; StJohn, D.H. Potency of High-Intensity Ultrasonic Treatment for Grain Refinement of Magnesium Alloys. *Scr. Mater.* **2008**, *59*, 19–22. [\[CrossRef\]](#)
10. Qian, M.; Cao, P. Discussions on grain refinement of magnesium alloys by carbon inoculation. *Scr. Mater.* **2005**, *52*, 415–419. [\[CrossRef\]](#)
11. Easton, M.; StJohn, D. Grain refinement of aluminum alloys: Part I. the nucleant and solute paradigms—A review of the literature. *Metall. Mater. Trans. A* **1999**, *30*, 1613–1623. [\[CrossRef\]](#)
12. Liu, Y.; Zhao, T.; Ju, W.; Shi, S. Materials discovery and design using machine learning. *J. Mater.* **2017**, *3*, 159–177. [\[CrossRef\]](#)
13. Agrawal, A.; Parijat, D.D.; Ahmet, C.; Gautham, P.B.; Alok, N.C.; Surya, R.K. Exploration of data science techniques to predict fatigue strength of steel from composition and processing parameters. *Integr. Mater. Manuf. Innov.* **2014**, *3*, 8. [\[CrossRef\]](#)
14. Wicker, J.G.; Cooper, R.I. Will it crystallise? Predicting crystallinity of molecular materials. *CrystEngComm* **2015**, *17*, 1927–1934. [\[CrossRef\]](#)
15. Fan, Z.; Wang, Y.; Xia, M.S. Enhanced heterogeneous nucleation in AZ91D alloy by intensive melt shearing. *Acta Mater.* **2009**, *57*, 4891–4901. [\[CrossRef\]](#)
16. Tiller, W.; Jackson, K.A.; Rutter, J.W.; Chalmers, B. The redistribution of solute atoms during the solidification of metals. *Acta Metall.* **1953**, *1*, 428–437. [\[CrossRef\]](#)
17. Maxwell, I.; Hellawell, A. A simple model for grain refinement during solidification. *Acta Metall.* **1975**, *23*, 229–237. [\[CrossRef\]](#)

18. Li, S.; Tang, B.; Zeng, D.B. Effects and mechanism of Ca on refinement of AZ91D alloy. *J. Alloys Compd.* **2007**, *437*, 317–321. [[CrossRef](#)]
19. Cheng, S.L.; Yang, G.C.; Fan, J.F.; Li, Y.J.; Zhou, Y.H. Effect of Ca and Y Additions on Oxidation Behavior of Az91 Alloy at Elevated Temperatures. *Trans. Nonferrous Met. Soc. China.* **2009**, *19*, 299–304. [[CrossRef](#)]
20. Masoudpanah, S.; Mahmudi, R. Effects of rare-earth elements and Ca additions on the microstructure and mechanical properties of AZ31 magnesium alloy processed by ECAP. *Mater. Sci. Eng. A* **2009**, *526*, 22–30. [[CrossRef](#)]
21. Easton, M.; StJohn, D. Grain refinement of aluminum alloys: Part II. Confirmation of, and a mechanism for, the solute paradigm. *Metall. Mater. Trans. A* **1999**, *30*, 1625–1633. [[CrossRef](#)]
22. StJohn, D.; Qian, M.; Easton, M.A.; Cao, P. The Interdependence Theory: The relationship between grain formation and nucleant selection. *Acta Mater.* **2011**, *59*, 4907–4921. [[CrossRef](#)]
23. Lu, H.; Wang, L.C.; Kung, S.K. Grain refining in A356 alloys. *J. Chin. Foundrym Assoc.* **1981**, *29*, 10–18.
24. Spittle, J.; Sadli, S. Effect of alloy variables on grain refinement of binary aluminium alloys with Al–Ti–B. *Mater. Sci. Technol.* **1995**, *11*, 533–537. [[CrossRef](#)]
25. Desnain, P.H.; Fautrelle, Y.; Meyer, J.L.; Riquet, J.P.; Durand, F. Prediction of Equiaxed Grain Density in Multicomponent Alloys, Stirred Electromagnetically. *Acta Metall. Mater.* **1990**, *38*, 1513–1523. [[CrossRef](#)]
26. Easton, M.; StJohn, D. An analysis of the relationship between grain size, solute content, and the potency and number density of nucleant particles. *Metall. Mater. Trans. A* **2005**, *36*, 1911–1920. [[CrossRef](#)]
27. Chai, G. Relation between grain size and coherency parameters in aluminium alloys. *Mater. Sci. Technol.* **1995**, *11*, 1099–1103. [[CrossRef](#)]
28. Easton, M.; Davidson, C.; John, D.S. Effect of alloy composition on the dendrite arm spacing of multicomponent aluminum alloys. *Metall. Mater. Trans. A* **2010**, *41*, 1528–1538. [[CrossRef](#)]
29. Easton, M.; StJohn, D. Partitioning of titanium during solidification of aluminium alloys. *Mater. Sci. Technol.* **2000**, *16*, 993–1000. [[CrossRef](#)]
30. Johnsson, M.; Backerud, L.; Sigworth, G.K. Study of the mechanism of grain refinement of aluminum after additions of Ti-and B-containing master alloys. *Metall. Trans. A* **1993**, *24*, 481–491. [[CrossRef](#)]
31. Lee, Y.; Dahle, A.K.; Stjohn, D.H.; Hutt, J.E.C. The effect of grain refinement and silicon content on grain formation in hypoeutectic Al–Si alloys. *Mater. Sci. Eng. A* **1999**, *259*, 43–52. [[CrossRef](#)]
32. Lee, Y.; Dahle, A.K.; Stjohn, D.H. The role of solute in grain refinement of magnesium. *Metall. Mater. Trans. A* **2000**, *31*, 2895–2906. [[CrossRef](#)]
33. Greer, A.L. Overview: Application of Heterogeneous Nucleation in Grain-Refining of Metals. *J. Chem. Phys.* **2016**, *145*, 211704. [[CrossRef](#)] [[PubMed](#)]
34. Qian, M.; Cao, P.; Easton, M.A.; McDonald, S.D.; Stjohn, D.H. An analytical model for constitutional supercooling-driven grain formation and grain size prediction. *Acta Mater.* **2010**, *58*, 3262–3270. [[CrossRef](#)]
35. Dantzig, J.A.; Rappaz, M. *Solidification*, 2nd ed.; EPFL Press: Lausanne, Switzerland, 2016.
36. Trivedi, R.; Kurz, W. Solidification microstructures: A conceptual approach. *Acta Metall. Mater.* **1994**, *42*, 15–23. [[CrossRef](#)]
37. Easton, M.; StJohn, D. Improved prediction of the grain size of aluminum alloys that includes the effect of cooling rate. *Mater. Sci. Eng. A* **2008**, *486*, 8–13. [[CrossRef](#)]
38. Shu, D.; Sun, B.; Mi, J.; Grant, P.S. A quantitative study of solute diffusion field effects on heterogeneous nucleation and the grain size of alloys. *Acta Mater.* **2011**, *59*, 2135–2144. [[CrossRef](#)]
39. Rappaz, M.; Thévoz, P. Solute diffusion model for equiaxed dendritic growth: Analytical solution. *Acta Metall.* **1987**, *35*, 2929–2933. [[CrossRef](#)]
40. Aaron, H.B. Diffusion-limited phase transformations: A comparison and critical evaluation of the mathematical approximations. *J. Appl. Phys.* **1970**, *41*, 4404–4410. [[CrossRef](#)]
41. Mueller, B.; Perepezko, J. The undercooling of aluminum. *Metall. Trans. A* **1991**, *18*, 1143–1150. [[CrossRef](#)]
42. Men, H.; Jiang, B.; Fan, Z. Mechanisms of grain refinement by intensive shearing of AZ91 alloy melt. *Acta Mater.* **2010**, *58*, 6526–6534. [[CrossRef](#)]
43. Günther, R.; Hartig, C.; Bormann, R. Grain refinement of AZ31 by (SiC) P: Theoretical calculation and experiment. *Acta Mater.* **2006**, *54*, 5591–5597. [[CrossRef](#)]
44. Arnberg, L.; Bäckerud, L.; Klang, H. Production and properties of master alloys of Al–Ti–B type and their ability to grain refine aluminium. *Metall. Technol.* **1982**, *9*, 1–6. [[CrossRef](#)]
45. Kailkhura, B.; Gallagher, B.; Kim, S.; Hiszpanski, A.; Han, Y.J. Reliable and explainable machine-learning methods for accelerated material discovery. *Comput. Mater.* **2019**, *5*, 1–9. [[CrossRef](#)]
46. Meredig, B.; Agrawal, A.; Kirklin, S.; Saal, J.E. Combinatorial screening for new materials in unconstrained composition space with machine learning. *Phys. Rev. B* **2014**, *89*, 094104. [[CrossRef](#)]
47. Gu, B.; Sheng, V.S.; Wang, Z.J.; Ho, D.; Li, S. Incremental learning for  $\nu$ -support vector regression. *Neural Netw.* **2015**, *67*, 140–150. [[CrossRef](#)]
48. Chen, T.; Guestrin, C. Xgboost: A scalable tree boosting system. In Proceedings of the 22nd ACM SIGKDD International Conference on Knowledge Discovery and Data Mining, San Francisco, CA, USA, 13–17 August 2016.

- 
49. Padula, D.; Simpson, J.D.; Troisi, A. Combining Electronic and Structural Features in Machine Learning Models to Predict Organic Solar Cells Properties. *Mater. Horiz.* **2019**, *6*, 343–349. [[CrossRef](#)]
  50. Yuan, R.; Liu, Z.; Balachandran, P.V.; Xue, D.Q.; Lookman, T. Accelerated discovery of large electrostrains in BaTiO<sub>3</sub>-based piezoelectrics using active learning. *Adv. Mater.* **2018**, *30*, 1702884. [[CrossRef](#)]